Departmental Papers (BE)   Department of Bioengineering

2006

A Joint Transformation and Residual Image Descriptor for Morphometric Image Analysis using an Equivalence Class Formulation

Sokratis Makrogiannis
University of Pennsylvania, makrogis@uphs.upenn.edu

Ragini Verma
University of Pennsylvania, vermar@uphs.upenn.edu

Bilge Karacali
University of Pennsylvania, karacalb@uphs.upenn.edu

Christos Davatzikos
University of Pennsylvania, davatzic@uphs.upenn.edu

Follow this and additional works at: http://repository.upenn.edu/be_papers

Part of the Bioimaging and Biomedical Optics Commons

A Joint Transformation and Residual Image Descriptor for Morphometric Image Analysis using an Equivalence Class Formulation

Abstract

Existing computational anatomy methodologies for morphometric analysis of medical images are often based solely on the shape transformation, typically being a diffeomorphism, that warps these images to a common template or vice versa. However, anatomical differences as well as changes induced by pathology, prevent the warping transformation from producing an exact correspondence. The residual image captures information that is not reflected by the diffeomorphism, and therefore allows us to maintain the entire morphological profile for analysis. In this paper we present a morphological descriptor which combines the warping transformation with the residual image in an equivalence class formulation, to characterize morphology of anatomical structures. Equivalence classes are formed by pairs of transformation and residual, for different levels of smoothness of the warping transformation. These pairs belong to the same equivalence class, since they jointly reconstruct the exact same morphology. Moreover, pattern classification methods are trained on the entire equivalence class, instead of a single pair, in order to become more robust to a variety of factors that affect the warping transformation, including the anatomy being measured. This joint descriptor is evaluated by statistical testing and estimation of class separation by classification, initially for 2-D synthetic images with simulated atrophy and subsequently for a volumetric dataset consisting of schizophrenia patients and healthy controls. Results of class separation indicate that this joint descriptor produces generally better and more robust class separation than using each of the components separately.

Disciplines

Bioimaging and Biomedical Optics | Biomedical Engineering and Bioengineering | Engineering

A Joint Transformation and Residual Image Descriptor for Morphometric Image Analysis using an Equivalence Class Formulation

Sokratis Makrogiannis, Ragini Verma, Bilge Karacali, and Christos Davatzikos
Section of Biomedical Image Analysis, Department of Radiology
University of Pennsylvania, Philadelphia, PA, 19104
{makrogis,vermar,karacalb,davatzic}@uphs.upenn.edu

Abstract

Existing computational anatomy methodologies for morphometric analysis of medical images are often based solely on the shape transformation, typically being a diffeomorphism, that warps these images to a common template or vice versa. However, anatomical differences as well as changes induced by pathology, prevent the warping transformation from producing an exact correspondence. The residual image captures information that is not reflected by the diffeomorphism, and therefore allows us to maintain the entire morphological profile for analysis. In this paper we present a morphological descriptor which combines the warping transformation with the residual image in an equivalence class formulation, to characterize morphology of anatomical structures. Equivalence classes are formed by pairs of transformation and residual, for different levels of smoothness of the warping transformation. These pairs belong to the same equivalence class, since they jointly reconstruct the exact same morphology. Moreover, pattern classification methods are trained on the entire equivalence class, instead of a single pair, in order to become more robust to a variety of factors that affect the warping transformation, including the anatomy being measured. This joint descriptor is evaluated by statistical testing and estimation of class separation by classification, initially for 2-D synthetic images with simulated atrophy and subsequently for a volumetric dataset consisting of schizophrenia patients and healthy controls. Results of class separation indicate that this joint descriptor produces generally better and more robust class separation than using each of the components separately.

1. Introduction

Methods falling under the general umbrella of computational anatomy are used to derive complex spatial maps of anatomical characteristics in normal and diseased popula-tions, using high-dimensional spatial transformations, often desired to be diffeomorphisms, which warp or spatially normalize these images to a common template [16, 13, 5, 17, 10, 1, 2, 3, 12] or vice versa. Measures computed from the shape transformation are used as image descriptors assuming that a perfect registration has been achieved between the images and the template, thereby relying on the accuracy of the registration algorithm to correctly estimate the shape. However, due to natural anatomical differences in human anatomy as well as changes induced by diseases, a perfect correspondence is hard to achieve via the warping transformation. Consequently, subsequent morphological analysis based solely on the transformation is limited, since it ignores morphological characteristics not captured by the transformation. The residual image captures information that is not reflected by the warping transformation hence, in conjunction with the shape transformation, it provides a means for deriving a complete morphological profile for analysis.

Herein we examine a morphological descriptor which combines the information from the warping transformation with the residual image, in an equivalence class formulation. Equivalence classes are formed by pairs of transformation and residual for different levels of smoothness of the warping transformation, and therefore of different residuals. These pairs belong to the same class as they jointly reconstruct the same anatomy. In this paper we restrict our attention to volumetric analysis only, hence we use a specific combination of the transformation and the residual, which warranties preservation of volumes, according to the work of [9]. The produced tissue density maps are based on the mass preservation principle during the warping operation, according to which the tissue density increases in the areas of contraction and decreases where extraction occurs. This can be carried out by combining a local measure of volume contraction/expansion provided by the Jacobian of the deformation field with the difference between the segmented normalized subject and template, a formulation that is significantly different from the Jacobian alone. According to

this formulation, an integration of the tissue density maps over any arbitrary anatomical region yields exactly the volume of this region in the individual under study, regardless of the warping transformation itself. Accordingly, comparisons of anatomical tissue volumes between different individuals are performed by comparing the respective tissue density maps. For example, brain atrophy in a particular brain structure will be reflected by reduced tissue density in that structure. We note, here, that a tissue density map has no relation with the physical density of the underlying tissue, but it is a mathematical construct used for morphological analysis.

Different transformations yield different tissue densities, for a given individual's anatomy. For example, applying the identity as transformation produces the original segmented image (one label for each tissue class; for the brain these would be gray matter, white matter and CSF). A completely conforming transformation corresponds to a tissue density map that follows exactly the morphology of the template and has values dependent on the tissue volumes of the respective individual. Varying levels of smoothness of the warping transformation are used to generate the elements of an equivalence class, aiming at rendering the resulting morphological descriptor robust to errors and unwanted variability emanating from the transformation process. For example, if an individual anatomy resembles the template, the shape transformation is likely to completely capture the individual's morphological subtleties. However, the opposite is true for an individual that is quite different from the template, for which trying to enforce correspondence via the shape transformation can introduce errors and noise. The distance between two anatomical images can then be defined by the distance of the respective equivalence classes, and could correspond to a distance derived from shape transformations of different smoothness properties for the two individuals.

In order to ultimately use these equivalence class descriptors for diagnostic purposes, we train pattern classification methods on equivalence classes instead of shape transformations or of single pairs of residual and transformation. The joint descriptor we propose is evaluated by statistical testing and estimation of class separation by classification, for 2-D synthetic images with simulated atrophy, and for a volumetric dataset consisting of schizophrenia patients and healthy controls. Results of class separation indicate that this joint descriptor produces generally better and more robust class separation than using each of the components separately.

In the next section the investigated image descriptor and its multiscale extension are detailed, followed by a brief description of the testing and validation methodology. Section 3 presents and discusses the experimental results on synthetic 2-D and real volumetric datasets. In the final sec-

tion are reported the contributions and future goals of our research.

2. Morphometric Analysis Framework

2.1. Joint Representation of Residual and Transformation using Tissue Density Maps

Let $S(.)$ and $T(.)$ be the subject and template images respectively. In the computational anatomy framework, a spatial normalization process is regularly employed that warps $T(.)$ to $S(.)$ or vice versa, and the following relation is derived

$$S(h(w)) = T(w) + D(w), \forall w \in \Omega_T, \quad (1)$$

where $h : \Omega_T \to \Omega_S$ is a mapping from the template Ω_T to the subject domain Ω_S, and $D(.)$ is the residual remaining after warping. Registration algorithms typically try to determine the deformation that minimizes some quantity related to the residual, under certain smoothness constraints. In the following paragraphs both the deformation and residual information are incorporated into a morphometric descriptor that originates from eq. 1. For reference, we compare results obtained via this morphological representation to those produced by the determinant of the Jacobian of deformation field [6], which provides a local measure of expansion or contraction of the template during the transformation and can therefore be used to measure the volume of a structure. The Jacobian-based descriptor performs well when the registration algorithm produces a sufficiently accurate deformation field.

As briefly described in the Introduction, we use tissue density maps to derive a morphological representation that reflects regional volumetrics, and is therefore a restricted case of a more general framework involving $h(.)$ and $D(.)$. In this paper, all of our experiments involve brain images, therefore three tissue density maps are generated: one for gray matter (GM), one for white matter (WM) and another one for cerebro-spinal fluid (CSF). The tissue density maps are calculated by multiplying each segmented and spatially normalized subject with the Jacobian of the deformation field. In other words, the binary mask of each tissue type is deformed and then multiplied by the Jacobian of the deformation field. This calculation is expressed by:

$$
\begin{aligned}
R_j(w) &= J(w) \cdot S_j(h(w)) \\
&= J(w) \cdot [T_j(w) + D_j(w)] \quad (2) \\
J(w) &= \det \nabla h(w) \\
&\quad h : \Omega_T \to \Omega_S
\end{aligned}
$$

where $S_j(h(.))$ denotes the indicator (binary) function of jth tissue of the spatially normalized image via the transformation $h(.)$, T_j the segmented j^{th} tissue of the template, $D_j(.)$ the difference image between the previous two and $J(.)$ the determinant of Jacobian of deformation field $h(.)$.

The representation of tissue density maps as expressed by eq. 2 incorporates the contraction/expansion estimate provided by the determinant of Jacobian of the transformation $J(.)$, plus the shape residual information $D_j(.)$ that is calculated from the region labels of the subject and template. As a result, although this descriptor cannot capture the intensity variations, it preserves the volume structure information that cannot be expressed by the warping transformation only. It is also worth noting that the number of density maps is equal to the number of tissue types for each subject, i.e. 3 for our brain experiments, but the overall dimensionality of the descriptor is approximately of equal order to that of the Jacobian-based feature, since the different density maps of a subject are only marginally overlapping.

Furthermore, eq. 2 produces an equivalence class determined from different pairs of transformations and residuals for the given representation $S(.)$ of a subject anatomy. The equivalence class $E(S)$ is defined as:

$$E(S) = \{[h(w), D(w)] : S(h(w)) = T(w) + D(w)\}, \quad (3)$$
$$h(.) \in \mathcal{T}, w \in \Omega_T,$$

where $\mathcal{T}$ is a family of transformations. This equivalence class representation can be interpreted as follows: in the feature domain of anatomical representations, which in our case are the tissue density maps, the registration algorithm that deforms the template to a subject forms a continuous curve, the origin of which is the template. This curve lies inside the hypersurface that is formed by all valid pairs of transformations and shape residuals that satisfy eq. 3. Different subjects produce different hypersurfaces in this domain; inter-subject distances are obtained from distances of respective hypersurfaces in this context. In principle, the estimation of a class dissimilarity requires the generation of all warping transformations and/or to solve an optimization problem in this domain of very high dimensionality to find the minimum distance. This represents a computationally very demanding problem. A more feasible approach is to generate some representative subsets of those classes and calculate their distances. These subsets are produced here by applying deformations of multiple levels of smoothness to each subject and calculating the tissue density maps.

The inter-subject distance may be readily calculated by the distances of the generated sub-classes. Our main premise in this context is that a more accurate estimate of the distance between different anatomies is determined by the distances of their respective equivalence classes. Different distance functions may be employed based on minimum, mean, or voting operations that can be incorporated into a classification scheme as described in the next section. Figure 1 illustrates the equivalence sub-classes of two subject images in the continuum of joint warping and residual representation. The dots correspond to the sub-class members produced by calculating tissue density maps over
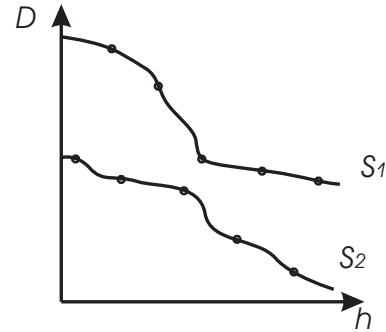

Figure 1. Example of the equivalence sub-classes produced by the spatial normalization of two subjects with varying degrees of smoothness in the representation domain provided by the tissue density maps.

deformation fields of varying rigidity. Those equivalence sub-classes are subsequently used for calculating the inter-individual distances in a statistical analysis framework.

2.2. Testing and Validation

In the following paragraphs we briefly describe the approaches that we used in order to assess the class separation capabilities of the presented descriptor.

Statistical t-test-The statistical significance of the image descriptor was initially evaluated by applying a t-test to the feature vectors coming from different subject groups [7]. The t-test is employed to estimate the distance between the mean values of two feature distributions. This was applied voxel-wise and the calculated p-values were geometrically averaged over the defined ROI.

Dimensionality Reduction by PCA-As described previously, the feature vectors may consist of the determinant of the deformation field Jacobian, or the tissue density maps. The dimensionality of this feature space is very high, therefore can not be handled efficiently in the subsequent stages of statistical analysis and pattern classification, especially given the limited availability of training data. A process is thus required to reduce the dimensionality of the feature vectors.

In this work the Principal Component Analysis algorithm is employed [7], that seeks the linear projections that represent the data optimally in terms of least-squares approximation. The dimensionality of data is reduced by selecting the directions of most extended spreads of the dataset.

Classification-The separation capabilities of the considered descriptors are compared in the context of classification accuracy. Therefore, pattern classifiers are built upon the two examined descriptors, to provide a common basis for comparisons.

IEEE
COMPUTER
SOCIETY

The k Nearest Neighbor (k-NN) scheme [4] is used for classification of our labeled data. The k-NN rule represents an extension of the nearest neighbor classification, where the argument of maximum posterior probability of the nearest prototype is sought. According to the k-Nearest Neighbor rule, the k closest samples are selected and a voting operation is applied next to assign a label to the unlabeled sample. Two classification rules were compared in the presented multi-scale context; first was the typical voting among the k-NNs and secondly a subsequent step was included that applies voting among the different samples that originate from the same subject. The latter rule should yield improved class separation and classification rates, assuming that the samples from the same subject form equivalence classes.

Cross Validation-The cross-validation of our methodology is carried out by the leave-one-out approach [8]. This is generally implemented by iteratively excluding one data sample from the training process and testing the classifier on this sample. This process is repeated for all the samples to assess the classification capabilities of the tested scheme. The final classification accuracy is calculated by the average performance of the tested schemes. It is worth noting that when cross-validating the multi-scale descriptors, all the members of the tested equivalence class are removed from the training set.

3. Experimental Results and Discussion

In this section we describe experiments that we conducted in order to assess the performance of the joint residual and deformation image descriptor, which characterizes the morphological changes in comparison with using the determinant of Jacobian of the deformation field that takes into consideration only the deformation. Those approaches were validated both on 2-D and 3-D datasets.

Synthetic 2-D Dataset-The initial synthetic dataset includes 20 subjects that represent normal cases and another 20 with simulated atrophy that was produced by the method proposed in [11]. The two examined image descriptors were compared in the context of statistical significance and classification accuracy.

A simple segmentation algorithm is applied to separate the tissue types. A thresholding with a low value is applied first to separate the subject from background. The image is thresholded next by a higher value to segment the white matter (WM) area. A connected component labeling operation is applied to the difference of the above two binary images and yields the gray matter (GM) and cerebro-spinal fluid (CSF) segmentation masks. Finally the white matter region is derived from the difference between the complete subject mask produced by the low threshold and the summation of WM and CSF masks. The registration part is car-

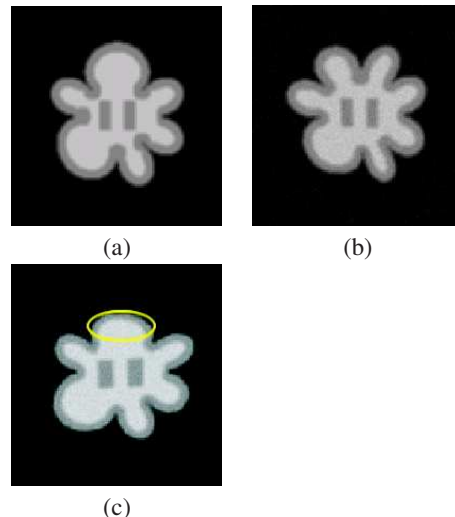(a)   (b)

(c)

Figure 2. (a) Template, (b) subject that corresponds to a normal case and (c) subject with simulated atrophy (indicated by the outlined area)

ried out by a 2-D energy minimization algorithm that applies gradient descent optimization on the image intensity information. The regularization parameter λ controls the smoothness of deformation field and consequently the registration accuracy. In particular smaller λs produce more flexible registrations.

In figure 2 are depicted (a) the template, (b) a subject image of a normal case, which was selected to have extended morphological variations from the template, and (c) a subject image of simulated atrophy. Moreover figure 3 depicts registration results from the subject without simulated atrophy to the template of figure 2 derived from deformation fields of varying smoothness i.e. different values of λ (left column) and the corresponding tissue density maps for the same parameter values. It becomes obvious that due to structural differences a perfect correspondence is difficult to be reached, that is the normalized subjects in figure 3 are still considerably different than the template in figure 2 therefore the residual image carries a considerable amount of information that needs to be included in the morphometric descriptor. The tissue density maps also show equivalent representations of the same subject at different scales. When a rigid deformation is applied, the residual mask $D_j(.)$ between the segmented normalized subject and the template carries most of the morphological information, while for more flexible transformations the volumetric feature of determinant of Jacobian $J(.)$ becomes more substantial.

The statistical significance estimates of the considered image descriptors were examined using the t-test and calculating the geometric average of p-values over a pre-defined
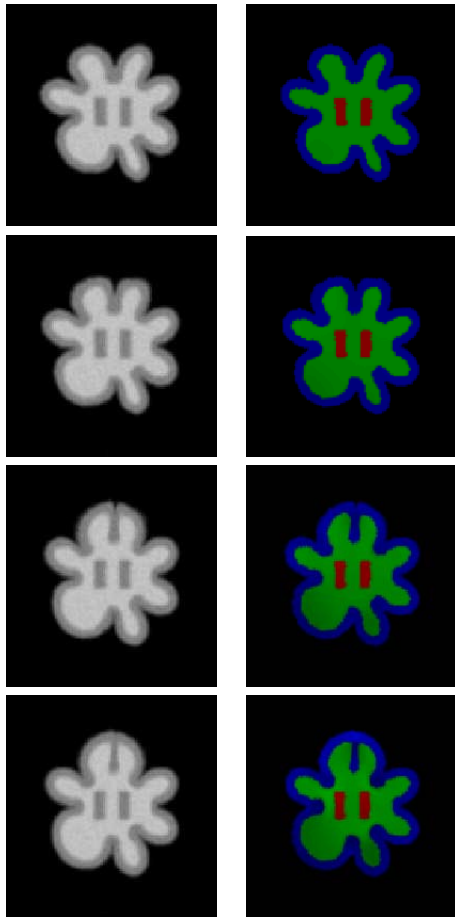
IEEE
COMPUTER
SOCIETY

Figure 3. Registration results from one of the simulated shapes to the template, for multiple levels of smoothness of the deformation field i.e. λ values (left column) and the corresponding color-coded tissue density maps (right column). In this example $\lambda = 2, 1/2, 1/8, 1/32$ from top to bottom.
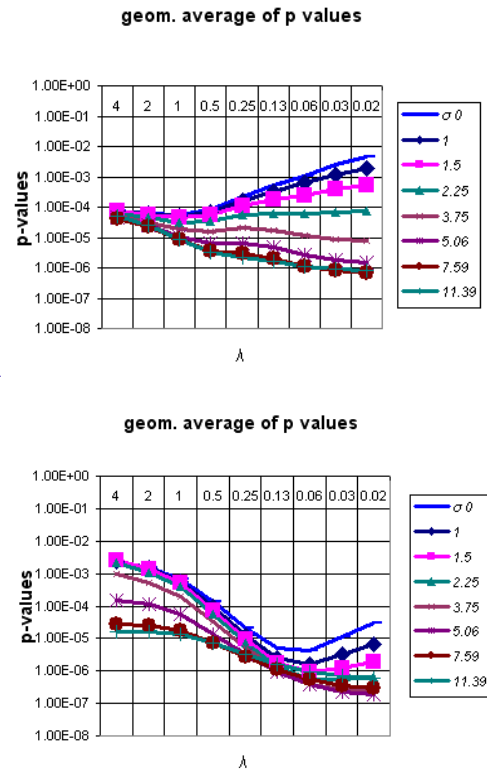

Figure 4. Statistical p-values of Jacobian (top) and tissue density map features (derived from t-test) (bottom) as a function of registration rigidity parameter for different standard deviations σ of Gaussian smoothing.

ROI that surrounds the area of simulated atrophy as in figure 2(c). The results produced by the Jacobian and the tissue density map-based descriptors for different λ values are depicted in figure 4. Due to the presence of noise in the employed dataset, the p-values were also estimated after applying Gaussian smoothing of variable standard deviations σ to the image descriptors. From those figures it becomes evident that the tissue density map-based descriptor regularly produces higher statistical significance i.e. lower p-values. It is also worth noting that the smoothing operation has improved those results since it reduces the noise.

The classification accuracy of the developed schemes was also examined. Several methodology variations were implemented and the results were finally compared on a common class separation basis as described in Section 2.2.

Figures 5 and 6 display the classification results of Jacobian and tissue density map descriptors after applying PCA to those descriptors and cross-validating the k-NN classification scheme using the leave-one-out approach. The classification performance is measured by the Classification Accuracy (CA) measure that is a weighted sum of true positive and true negative fractions. The main distinction in this framework is the use of data from one or multiple scales -i.e. levels of smoothness- of the deformation field. This level of smoothness is controlled by the λ parameter here. Two classification rules were also compared in the multi-scale context to implicitly validate the construction of equivalence classes as explained in Section 2.1. In figure 5 the classification is calculated for the Jacobian-based descriptor and separate (figure 5(a)) or combined multiple scales of smoothness of the transformation (figure 5(b)). Figure 6 displays the corresponding results from the tissue density map-based features. The multi-scale framework was compared to the average classification performance of the single scale counterparts (figures 5(b) and 6(b))
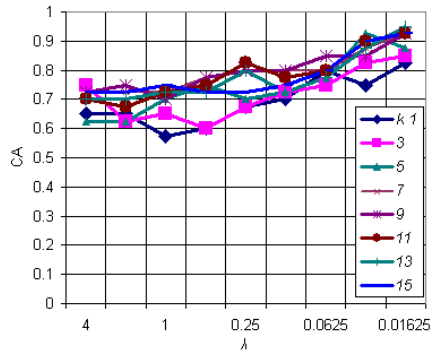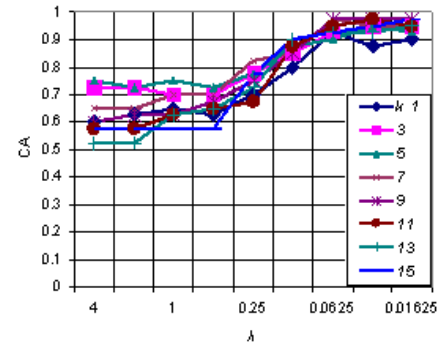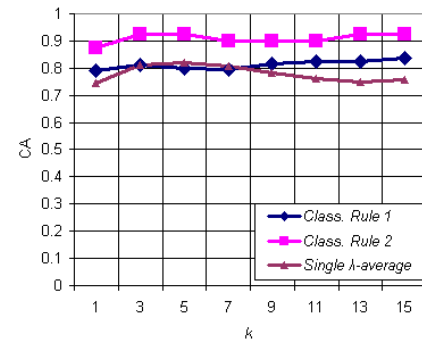
(a)
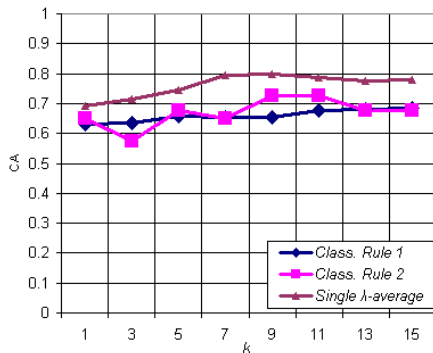
(b)

Figure 5. Classification rates produced by the Jacobian-based descriptor for (a) single and (b) multiple λ values compared to the average performance of single scale representation vs the number of nearest neighbors k (bottom).

(a)

(b)

Figure 6. Classification rates produced by the tissue density map-based descriptor for (a) single and (b) multiple λ values compared to the average performance of single scale representation vs the number of nearest neighbors k.

as well. From figure 5(a) it is inferred that for the case of Jacobian-based descriptor the classification accuracy is improved when more flexible deformation fields are employed, which is normal since this descriptor relies on the registration accuracy. Besides that, the use of multiple scales does not improve its classification performance as depicted in figure (5(b)), because this descriptor doesn't generate equivalence classes. On the other hand, the multi-scale version of the tissue density map-based descriptor produces better separation than single scale processing, that is further enhanced when the different samples from the same subject are grouped in the nearest neighbor finding process (see second classification rule in figure 6(b)). Those observations indicate that the tissue density maps divide the feature space into equivalence classes.

Real 3-D Dataset-The proposed morphometric descriptor was also tested on a volumetric dataset that included 38 normal controls and 23 schizophrenia patients. The seg-

mentation into the three tissue types (white matter, gray matter and cerebro-spinal fluid) was carried out by [14]. The spatial normalization was accomplished by a 3-D high dimensional and hierarchical deformable registration algorithm [15]. The resulting deformation fields were subsequently downsampled by a factor of 4 to reduce the computational load and the tissue density maps were calculated next. The multi-scale hierarchy was constructed by imposing different levels of smoothness in the image warping mechanism. The tissue density maps are calculated next at multiple scales, i.e. levels of smoothness ls, given the deformation fields. The feature vector is constructed by multiplying the tissue density maps with a mask of all voxels with at least one non-zero tissue density value in our dataset and concatenating the results from the different tissue types. The dimensionality of the feature vectors is reduced by PCA and then they are processed in the k-NN classification context using the leave-one-out approach as described in the previous sections.

In figure 7 are displayed (a) the images of a subject, (b) the template, (c) the final registration result by [15] and (d) the resulting residual image from the transformation. A perfect registration cannot be achieved due to extensive structural differences as shown in figure 7(d), therefore an exclusively deformation-based descriptor cannot represent the morphological properties of the subjects with sufficient accuracy. In addition, figure 8 depicts four generated deformation fields of varying rigidity and the resulting tissue density maps. It is obvious that the deformation fields become more rigid and the tissue density maps smoother as the number of smoothing iterations -or equivalently the scale index- increases (from bottom to top). The classification rates are depicted in figure 9 for single and multiple scales and by the same classification rules as in the 2-D experiment. From figure 9 we observe that the multi-scale representation considerably improves the class separation especially for smaller values of k. Besides that, the slightly better performance of the second classification rule implies the construction of equivalence classes by the tissue density-based feature (Section 2.1).

Discussion-The results obtained from 2-D and 3-D experiments are in general consistent with each other on the basis of comparing image descriptors, multiple vs single scale representations and classification rules. The lower classification rates of the volumetric data are attributed to the increased spatial complexity of the real structures and their higher dimensionality. Nevertheless the main purpose of the employed simple classification scheme is to estimate the class separation, validate our results and serve as a common basis for comparisons between the examined descriptors. Our assessment of the experimental results mostly indicated that the tissue density map descriptor produces better classification rates than the Jacobian features overall. Moreover, for the case of tissue density maps, the use of multiple scales improves the classification accuracy, presumably because of the more accurate estimation of inter-individual distances provided by the equivalence subclasses.

4. Conclusions

A volume preserving image descriptor for computational morphometry was presented in this work. This descriptor incorporates shape and residual information derived from a spatial normalization process by calculation of the tissue density maps. Several degrees of rigidity in the deformation field were also tested and it was indicated that the use of multiple levels of smoothness of deformation enhances the separation between different groups. The validation process included voxel-wise statistical testing and estimation of the class separation by classification. This methodology was tested on synthetic 2-D and real 3-D data as well.
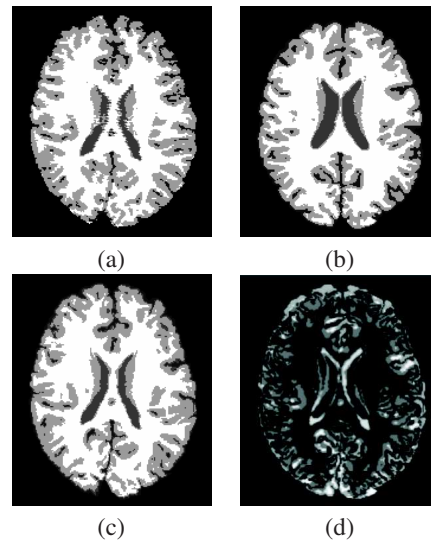

Figure 7. (a) One subject, (b) the template, (c) the normalized subject after the application of the registration algorithm, and (d) the residual image between (b) and (c).

Our future goals include the introduction of a manifold modelling approach of the tissue density maps by sub-space decomposition to learn distances between different brain anatomies and the investigation of alternate multiresolution extensions of the proposed descriptor based on a non-linear scale-space or wavelet decomposition structure.

References

[1] J. Ashburner and K. J. Friston. Voxel-based morphometry: the methods. *Neuroimage*, 11(6):805–821, 2000. 1

[2] G. E. Christensen, S. C. Joshi, and M. I. Miller. Volumetric transformations of brain anatomy. *IEEE Transactions on Medical Imaging*, 16(6):864–877, 1997. 1

[3] M. K. Chung, K. J. Worsleyb, T. Paus, C. Cherif, D. L. Collins, J. N. Giedd, J. L. Rapoport, and A. C. Evans. A unified statistical approach to deformation-based morphometry. *NeuroImage*, 14(3):595–606, 2001. 1

[4] B. V. Dasarathy, editor. *Nearest Neighbor (NN) Norms: NN Pattern Classification Techniques*. IEEE Computer Society, Washington, DC, 1991. 4

[5] C. Davatzikos. Mapping of image data to stereotaxic spaces. *Human Brain Mapping*, 6:334–338, 1998. 1

[6] C. Davatzikos, M. Vaillant, S. Resnick, J. L. Prince, S. Levotsky, and N. Bryan. A computerized approach for morphological analysis of the corpus callosum. *Journal of Computer Assisted Tomography*, 20:88–97, 1996. 2

[7] R. O. Duda, P. E. Hart, and D. G. Stork. *Pattern Classification*. Wiley-Interscience, 2001. 3

[8] K. Fukunaga and D. M. Hummels. Leave-one-out procedures for nonparametric error estimates. *IEEE Transactions on Pattern Analysis and Machine Intelligence*, 11(4):421–423, 1989. 4
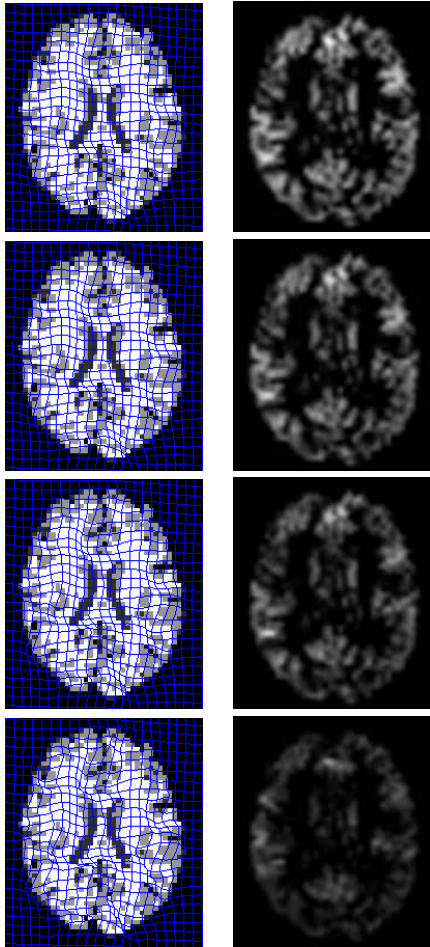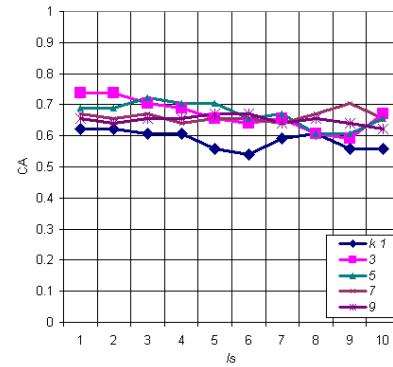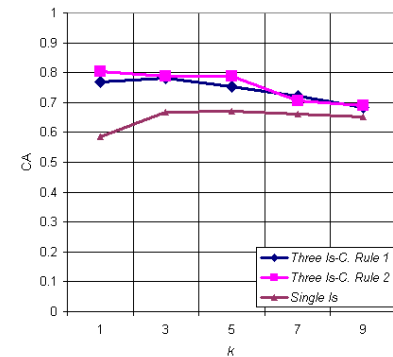
Figure 8. Deformation fields of varying registration rigidity (left column) and the corresponding tissue density maps of gray matter (right column).

(a)

(b)

Figure 9. Classification rates for (a) single and (b) multiple levels of smoothness (ls) using different classification rules and multiple scales compared to the average performance of single scale representation vs the number of nearest neighbors k for the 3-D dataset.

 [9] A. F. Goldszal, C. Davatzikos, D. L. Pham, M. X. H. Yan, R. N. Bryan, and S. M. Resnick. An image-processing system for qualitative and quantitative volumetric analysis of brain images. *Journal of Computer Assisted Tomography*, 22(5):827–837, 1998. 1

[10] P. Golland, W. E. L. Grimson, M. E. Shenton, and R. Kikinis. Deformation analysis for shape based classification. *Lecture Notes in Computer Science*, 2082:517–530, 2001. 1

[11] B. Karacali and C. Davatzikos. Estimating topology preserving and smooth displacement fields. *IEEE Transactions on Medical Imaging*, 23(7):868–880, 2004. 4

[12] Z. Lao, D. Shen, Z. Xue, B. Karacali, S. M. Resnick, and C. Davatzikos. Morphological classification of brains via high-dimensional shape transformations and machine learning methods. *Neuroimage*, 21(1):46–57, 2003. 1

[13] M. Miller, A. Banerjee, G. Christensen, S. Joshi, N. Khaneja, U. Grenander, and L. Matejic. Statistical methods in computational anatomy. *Statistical Methods in Medical Research*, 6(3):267–299, 1997. 1

[14] D. L. Pham and J. L. Prince. Adaptive fuzzy segmentation of magnetic resonance images. *IEEE Transactions on Medical Imaging*, 18(9):737–752, 1999. 6

[15] D. Shen and C. Davatzikos. Hammer: Hierarchical attribute matching mechanism for elastic registration. *IEEE Transactions on Medical Imaging*, 21(11):1421–1439, 2002. 6, 7

[16] P. M. Thompson, D. MacDonald, M. S. Mega, C. J. Holmes, A. C. Evans, and A. W. Toga. Detection and mapping of abnormal brain structure with a probabilistic atlas of cortical surfaces. *Journal of Computer Assisted Tomography*, 21(4):567–581, 1997. 1

[17] A. W. Toga and P. M. Thompson. The role of image registration in brain mapping. *Image and Vision Computing*, 19(1):3–24, 2001. 1